Oxygen and carbon stable isotopes of *Mytilus galloprovincialis* Lamarck, 1819 shells as environmental and provenance proxies

Stefania Milano[a,b*]; Bernd R. Schöne[b]; Igor Gutiérrez-Zugasti[c]

[a] Department of Human Evolution, Max Planck Institute for Evolutionary Anthropology, Deutscher Platz 6, 04103 Leipzig, Germany
[b] Institute of Geosciences, University of Mainz, Johann-Joachim-Becherweg 21, 55128Mainz, Germany
[c] Instituto Internacional de Investigaciones Prehistóricas de Cantabria (Universidad de Cantabria, Gobierno de Cantabria, Banco Santander), Edificio Interfacultativo, Avda. Los Castros s/n., 39005 Santander, Spain

* Corresponding author. Email: stefania_milano@eva.mpg.de

Abstract

Mollusc shell stable isotopes are commonly used to reconstruct past environmental conditions. However, despite being abundant components of natural and anthropogenic fossil accumulations, the geochemical composition of mussel shells (*Mytilus* spp.) has rarely received attention in palaeoenvironmental studies. This study tests the suitability of oxygen isotopes ($\delta^{18}O_s$) of *M. galloprovincialis* as palaeothermometer. For one year, mussels and water samples were collected twice a month from Berria Beach, in Northern Spain. The geochemical data of the shells indicate that water temperatures can be reconstructed with an average offset of 1.2 ± 0.7°C with respect to the measured values. Furthermore, no prolonged shell growth cessations are observed. These results validate *M. galloprovincialis* as reliable recorders of seasonal water temperature fluctuations, supporting their use in palaeoenvironmental studies. In addition, further shell and

water collections were carried out in the upper and lower areas of a nearby estuary. The geochemical analyses of these shells were aimed to test whether oxygen and carbon stable isotopes ($\delta^{13}C_s$) may be used as novel proxies to identify the shell provenance at local scale. The results show that the $\delta^{18}O_s$ vs. $\delta^{13}C_s$ correlation direction varies along the coast-upper estuary geographical gradient, suggesting it to be a potential new proxy to distinguish between marine and estuarine mussel specimens.

Keywords: Mediterranean mussel; Northern Spain; Palaeoenvironmental reconstructions; Geochemistry; Proxy calibration; Provenance

1. Introduction

Mollusc shells are abundant remains in paleontological and archaeological accumulations worldwide. Their presence reflects both their extraordinary preservation potential and their tight connection with the evolution of our species since prehistoric times. In fact, besides natural aggregations, numerous archaeological sites contain large amounts of shell remains ('shell middens'). In human history, molluscs have played an important role primarily as easily accessible food resources but also as raw materials for various types of artefacts such as personal ornaments and tools, e.g., scrapers and fish hooks (Vanhaeren and d'Errico, 2005; Marean et al., 2007; Flores et al., 2016).

The geochemical properties of the shell calcium carbonate offer insights into the environmental conditions occurring at the time when the shells were built by the molluscs (Jones, 1983; Marchitto et al., 2000; Schöne, 2008). Among the different existing proxies, the oxygen stable isotope ratio of marine shells ($\delta^{18}O_s$) is a well-established palaeothermometer that allows highly-resolved water temperature reconstructions during time intervals prior to any instrumental record (Schöne and Gillikin, 2013; Gutiérrez-Zugasti et al., 2015). The incorporation of oxygen isotopes from the surrounding water into the shell is a temperature-dependent fractionation process. Through specific equations using the oxygen isotope value of the water ($\delta^{18}O_w$) and the $\delta^{18}O_s$, accurate estimations of the water temperature at the time of shell deposition are achieved (Epstein, 1953; Grossman and Ku, 1986).

Molluscs deposit the shell throughout their life. By using a high-resolution sampling approach on individual shells, it is possible to reconstruct the water temperature fluctuation at annual, seasonal and even weekly resolution (Schöne et al., 2004; Hallmann et al., 2009; Gutiérrez-Zugasti et al., 2015). Furthermore, the temperature reconstruction of the last shell portion formed just before death can give important information in archaeological contexts as it can be used to determine the season of shellfish collection and therefore human dietary habits (Mannino et al., 2007; Burchell et al., 2013; Prendergast et al., 2016).

Although *Mytilus* spp. are abundant in the archaeological record, there is lack of specific modern calibration studies testing the suitability of representatives of this genus for palaeoenvironmental reconstructions. The current study is based on modern *M. galloprovincialis* shell collection and water sampling. Geochemical analyses of the shells are used to assess the timing of shell growth and the environmental factors imprinted in the carbonate structure.

Furthermore, the wide range of habitat tolerance of mussel species that promotes their abundance in various aquatic habitats (from marine to freshwater) arouses interest over the shell provenance. Being able to identify the specific area where fossil shells were growing represents a significant advance in the interpretation of the $\delta^{18}O_s$ data for temperature reconstructions and in the understanding of archaeological accumulations of coastal and inland sites. The current study applies geochemical analyses on the abundant marine and estuarine *M. galloprovincialis* to test if oxygen and carbon ($\delta^{13}C_s$) stable isotopes can be used as a provenance proxy.

2. Background

2.1 Study area

The present study focuses on *M. galloprovincialis* shells collected from Cantabria, in the north of the Iberian Peninsula (Fig. 1). This region is characterized by a humid and temperate climate. The North Atlantic oceanic air masses, encountering the geographical barrier of the Cordillera Cantábrica mountain range that prevents any movement further inland towards the Iberian Peninsula, have a major influence on the climate of the region. The annual air temperature ranges between ca 9–10 °C and 20–22 °C, with an average around 15–16 °C. The annual precipitation is ca 1200 l/m^2, with drier conditions during summer and wetter conditions during the rest of the year (Source: AEMET, Agencia Estatal de Meteorología; http://www.aemet.es). The coasts of Cantabria are characterized by considerable tidal variations, whose amplitude ranges, on average, between 2 and 4 m (Pérez and Canteras, 1993). The seawater temperature ranges between ca 11°C and 24 °C, with an annual average of 16 °C (data from the SeaDataNet Pan-European infrastructure for ocean and marine data management; https://www.seadatanet.org/). The surface water

circulation in the Cantabrian Sea (southern Bay of Biscay) is strongly modulated by the seasonal wind direction. During autumn, winter and spring the circulation is dominated by eastward currents, whereas in summer currents are flowing mainly in the opposite direction (Botas et al., 1989). As for other temperate seas, water stratification occurs primarily in spring and summer with a gradual appearance of a thermocline between 20 and 50 m (Botas et al., 1989). Upwelling events of the cold and salty Eastern North Atlantic Central Water (ENACW) are particularly intense and frequent during the summer months (Álvarez et al., 2010; Álvarez et al., 2011). Near the coasts, the surface waters are also influenced by the contribution of 28 major rivers supplying water of continental origin (Prego et al., 2008).

2.2 Mytilus galloprovincialis ecology

M. galloprovincialis Lamarck, 1819, also known as Mediterranean mussel, is a sibling species of *M. edulis* and *M. trossulus*. Among them, *M. galloprovincialis* is the most widely spread species. In Europe, it is found throughout the Mediterranean Sea and northeast Atlantic Ocean (Barsotti and Meluzzi, 1968; Sanjuan et al., 1997; Hilbish et al., 2000). It also inhabits the northeast Pacific coasts from California to Mexico and the coasts of Chile, South Africa, Australia and Japan (McDonald and Koehn, 1988; McDonald et al., 1991). Typically, *M. galloprovincialis* lives in the intertidal and shallow subtidal zones anchored to rocks (Seed and Suchanek, 1992). The strong byssal attachment allows the mussels to withstand considerable wave stress, supporting the colonization of habitats characterized by high hydrodynamic energy (Waite, 1992). Furthermore, because of their tolerance against a wide range of salinity levels, these bivalves are also commonly found in estuaries and hyposaline environments (Seed, 1992; Soto et al., 1995; Diz and Presa, 2009). As many other species of bivalves, the Mediterranean mussels are suspension feeders

(Maire et al., 2007). Their lifespan generally ranges between two to four years (Abada-Boudjema and Dauvin, 1995; Okaniwa et al., 2010), with the spawning season depending on the geographic locality (i.e., during spring and early summer in NW Spain; Villalba, 1995).

The shell of *M. galloprovincialis* is characterized by a dark colour (Fig. 2A), ranging from blue to black, and it is formed by two calcium carbonate polymorphs. The outer shell layer is composed of calcite organized in prismatic microstructures, whereas the inner shell layer is made of nacre (aragonite) (Fig. 2B-C); Taylor et al., 1969; Lutz, 1976; Feng et al., 2000). As for other intertidal species, mussels are reported to grow their shells mostly during high tide, when continuously submerged by seawater (Richardson, 1989; Okaniwa et al., 2010; Lobbia, 2012). Shell deposition has been observed to vary seasonally, with slower growth occurring during the cold season (Richardson et al., 1990; Okaniwa et al., 2010; Lobbia, 2012). However, previous studies also observed a decrease in shell growth rate during the summer months, suggesting that the deposition may depend on the local hydrological conditions (Peharda et al., 2007).

3. Materials and methods

3.1 Shell collection and preparation

A total of 220 *M. galloprovincialis* specimens were collected from Berria Beach (43°27′54.5″N, 3°27′8.5″W; Fig. 1), on average, twice per month from 14 December 2016 to 19 December 2017. Together with the shells, water samples were collected for $\delta^{18}O$ and $\delta^{13}C_{DIC}$ (Dissolved Inorganic Carbon $\delta^{13}C$) analyses, and stored in 30 ml airtight polyethylene bottles (HDPE) and 40-ml glass bottles with no headspace at ca. 4 °C until measurement. The samples for $\delta^{13}C_{DIC}$ were injected with $CuSO_4$ (copper sulfate) to stop bacterial activity in the water. This locality was chosen as a

representative for the marine habitat. Following the same periodicity, water samples were retrieved from two additional localities: a lower estuarine site near Montehano (43°25′36.4″N, 3°29′27.2″W; Fig. 1) and an upper estuarine site near the town of Carasa (43°22′22.8″N, 3°28′14″W; Fig. 1). Specimens from these two localities were gathered on the last collection event, i.e., on 19 December 2017. On the same date, shells were collected at two different spots at Berria Beach: in the low intertidal zone (as for the rest of the annual collection) and in the high intertidal zone. In the low intertidal zone, the targeted mussel population was located at same height of the mean tide level, whereas, in the high intertidal level, the molluscs were subjected to slightly longer emersions during low tides. The soft tissues were removed immediately after collection, and the shells air-dried and stored in plastic bags for further analyses. At each collection event, water temperature was determined with a digital thermometer (Hanna HI 93532). Salinity was measured in the laboratory at the University of Cantabria (Spain) using a conductivity meter (WTW Cond 330i).

In this study, two carbonate powder sampling strategies were used. The first method was applied to the shells collected from Berria Beach throughout the twelve-month period. The ventral margins (calcite) of ten shells from each collection event were micromilled using a diamond-coated cylindrical bit (1 mm diameter; Komet/Gebr. Brasseler GmbH & Co. KG, model no. 835 104 010) mounted on a Rexim Minimo drill with a speed of 1000 min^{-1}. The milling depth was about 200 µm for all the specimens. The aim was to sample the last shell portion deposited immediately prior to collection, to relate its geochemical composition to the environmental data and ultimately to interpret the timing of seasonal shell growth. The second sampling strategy was applied to three shells per site collected on 19 December 2017 (last collection event). In this case, a protective layer of JB KWIK epoxy resin was applied along the axis of shell maximum growth, and sections of about 2.5 mm were cut from that axis using an IsoMet Low Speed Precision Cutter (Fig. 2A-B).

After mounting on microscope slides, the sections were ground on Buehler silicon carbide papers of different grit size (600, 1200, 2500, 4000). After each grinding step, the samples were rinsed in an ultrasonic bath for about 3 minutes and subsequently, they were polished on a Buehler VerduTex cloth with a 3 μm diamond suspension. The outer shell layers were sequentially micromilled for carbonate powder using a 300 μm-diameter conical bit (Komet/Gebr. Brasseler GmbH & Co. KG, model no. H52 104 003) mounted on a Rexim Minimo drill with a speed of with a speed of 1000 min^{-1}. For each shell section, ca. 30 calcite samples were produced. The samples were drilled ca 250 μm apart from each other.

To confirm *M. galloprovincialis* shell microstructural organization, the sections were analysed using a 3rd generation Phenom Pro desktop Scanning Electron Microscope (LOT-QuantumDesign GmbH Darmstadt, Germany) at the University of Mainz (Fig. 2C). Furthermore, their mineralogy was investigated using a WITec alpha 300 R (WITec GmbH, Germany) confocal Raman microscope at the Alfred Wegener Institute for Polar and Marine Research, Germany. A scan with a spatial resolution of 250 μm was performed at the interface of the two shell layers (Fig. 2C). The scan was carried out using a 488 nm diode laser and a spectrometer (UHTS 300, WITec, Germany) was used with a 600 mm^{-1} grating, a 500 nm blaze and an integration time of 0.1 s.

3.2 Stable isotope analyses

Shell carbonate powder samples were measured at two different laboratories, the University of Mainz (henceforth JGU) and the Department of Human Evolution, Max Planck Institute for Evolutionary Anthropology (henceforth MPI-EVA). At JGU, carbonate powder samples (N = 80; ranging between 60-130 μg) were dissolved in He-flushed borosilicate exetainers at 72 °C using a water-free phosphoric acid. The released CO_2 gas was then measured in continuous flow mode

with a ThermoFisher MAT 253 gas source isotope ratio mass spectrometer (CF-IRMS) coupled to a GasBench II. At MPI-EVA, samples (N = 476; ranging between 40-80 µg) were dissolved at 70 °C using a Kiel IV automated carbonate preparation device and CO_2 gas were then measured with a ThermoFisher MAT 253 Plus CF-IRMS. At JGU, stable isotope ratios were calibrated against an NBS-19 calibrated Carrara Marble ($\delta^{13}C$ = +2.01 ‰; $\delta^{18}O$ = −1.91 ‰) distributed by IVA Analysentechnik GmbH & Co. KG, whereas at MPI-EVA, data were calibrated against an IAEA-603 calibrated Carrara marble ($\delta^{18}O$= −1.64 ‰; $\delta^{13}C$= +1.87 ‰). Results are reported in per mil (‰) relative to the Vienna Pee-Dee Belemnite (VPDB) standard. At JGU, the average precision error (1σ; computed from eight injections per sample) was better than 0.05‰ for $\delta^{18}O$ and 0.03 ‰ for $\delta^{13}C$, and the long-term accuracy based on blindly measured NBS-19 samples (N = 421) was better than 0.04 ‰ for $\delta^{18}O$ and 0.03 ‰ for $\delta^{13}C$. At MPI-EVA, the average precision error (1σ; computed from eight measurements per sample) was better than 0.05‰ for $\delta^{18}O$ and 0.03 ‰ for $\delta^{13}C$, and the long-term accuracy based on blindly measured IAEA-603 samples (N = 268) was better than 0.05 ‰ for $\delta^{18}O$ and 0.03 ‰ for $\delta^{13}C$. Note that no correction was applied for differences in fractionation factors of the reference material (calcite) and shell aragonite; for details see Füllenbach et al. (2015).

The water sample $\delta^{18}O$ ($\delta^{18}O_w$) analysis was performed in duplicate by the equilibration technique using a Europa Scientific 20-20 CF-IRMS interfaced with an ANCA-GSL elemental analyser at the Iso-Analytical facilities, United Kingdom. The samples were measured against three reference standards. The first standard being IA-R063 with $\delta^{18}O_{VSMOW}$ = −0.41 ‰, the second IA-R065 with $\delta^{18}O_{VSMOW}$ = −33.57 ‰ and the third IA-R064 with $\delta^{18}O_{VSMOW}$ = −12.34 ‰. The average external precision was better than 0.04 ‰. The dissolved inorganic carbon $\delta^{13}C_{DIC}$ analysis of the water samples was performed in duplicate by the equilibration technique using a Europa

Scientific 20-20 CF-IRMS at the Iso-Analytical facilities as well. The reference gas used was IA-CO2-7 ($\delta^{13}C = -38.48$ ‰ vs. VPDB) and the average external precision was better than 0.06 ‰.

3.3 $\delta^{18}O_s$ prediction and temperature reconstruction

In order to test whether the shells of *M. galloprovincialis* are deposited in isotopic equilibrium with the seawater, the $\delta^{18}O_s$ of the ventral margins of the specimens collected from Berria Beach on fortnightly basis were compared with the predicted $\delta^{18}O_s$ values calculated using the calcite fractionation equations by Friedman and O'Neil (1977) (Fig. 3):

(1) $1000\ln\alpha = (2.78 \times 10^6 / T^2) - 2.89$

(2) $\alpha = (1000 + \delta^{18}O_{s\,(SMOW)}) / (1000 + \delta^{18}O_{w\,(SMOW)})$

where α is the water-calcite fractionation factor, T is the temperature recorded (expressed in Kelvin) and SMOW is the Vienna Standard Mean Ocean Water unit for isotope ratios.

Eqs. (1) and (2) were subsequently used to reconstruct the seawater temperatures in Berria Beach using both the shell ventral margins and the specimens sampled sequentially. For this purpose, two different $\delta^{18}O_w$ values were used in Eq. (2). The first value used was the annual average measured during the local water collections, $\delta^{18}O_w = -0.03$ ‰. However, such a negative value is not generally expected to reflect fully marine conditions. For instance, the $\delta^{18}O_w$ was previously measured on a monthly basis at Langre Beach (ca 15 km west of Berria Beach) by Gutiérrez-Zugasti et al. (2017). Their results showed that the annual average $\delta^{18}O_w$ is +0.90 ‰ (ranging between +0.55 ‰ and +1.19 ‰). This value was adopted in the temperature reconstruction equations presented in this study. Further discussion on Berria Beach $\delta^{18}O_w$ are presented in the section 5.1.

4. Results

4.1 Water physical data and geochemistry

The water measurements in Berria Beach indicate that the sea surface temperature (SST) throughout the year ranged between 11.7 °C and 20.8 °C and the salinity was rather constant, ranging between 34.3 PSU and 36.3 PSU (Table 1). Similar water temperature ranges were recorded at Montehano and Carasa, but salinity was lower and its variance higher, especially at Carasa (Table 1). The water data measured at Berria Beach on 5 December 2017 were precluded from further analyses, because salinity levels differed significantly from the rest of the samples (Table 1), suggesting a transitory freshwater input, possibly due to heavy rainfall. In fact, on this particular day, the tide was extremely low and the water was collected in a water pool between rocks that could have been affected by the rainy weather occurring at that time.

At Berria Beach, the average annual water $\delta^{18}O$ value equalled −0.03 ‰ and was characterised by a relatively small seasonal variation (Table 1). Similar values were observed in Montehano (average $\delta^{18}O_w$ = −0.04 ‰), whereas the average $\delta^{18}O$ value at Carasa was more negative (−1.57 ‰). The $\delta^{13}C_{DIC}$ values at Berria Beach ranged between −5.59 ‰ and −2.21 ‰, with more negative values occurring in the cold months (Table 1). A similar range occurred at Montehano, whereas at Carasa, values tended to be lower, i.e., they ranged between −11.66 ‰ and −3.99 ‰.

The correlation between salinity and $\delta^{18}O_w$ increased from the marine environment toward the estuarine localities. The same applies to the correlation between salinity and SST, salinity and $\delta^{13}C_{DIC}$ and between $\delta^{13}C_{DIC}$ and $\delta^{18}O_w$ (Table 2).

4.2 Shell oxygen isotopes and temperature reconstructions

The measured $\delta^{18}O$ values at the ventral margin of specimens collected at Berria Beach were characterised by some degree of variance, with higher values (maximum $\delta^{18}O_s$ = +1.71 ‰) during the cold months and lower values during the warm season (minimum $\delta^{18}O_s$ = −0.12 ‰; Table 3). Similar to the ventral margins, the shells from Berria sampled sequentially show $\delta^{18}O_s$ values between −0.65 ‰ and +1.93 ‰. The same applies to the specimens collected in the high intertidal zone ($\delta^{18}O_s$ between and −0.70 ‰ and +1.67 ‰). A tendency toward overall lower values was recorded in the estuarine localities (Montehano $\delta^{18}O_s$ between −1.31 ‰ and +1.87 ‰; Carasa $\delta^{18}O_s$ between −1.98 ‰ and +0.02 ‰; Table 4).

The predicted $\delta^{18}O_s$ values near the ventral margin of specimens from Berria Beach using Eqs. (1), (2) and $\delta^{18}O_w$ = −0.03 ‰ had a sinusoidal pattern that followed the measured $\delta^{18}O_s$ values (Fig. 3). However, between the two data series, a significant offset was apparent. In fact, the measured $\delta^{18}O_s$ were lower by, on average, 0.82 ± 0.31 ‰ (Root Mean Square Error = 0.90 ‰) than the predicted ones (Fig. 3A). When adopting $\delta^{18}O_w$ = +0.90 ‰, the offset was significantly reduced to 0.25 ± 0.17 ‰ (RMSE = 0.30 ‰), indicating that shell growth occurred in isotopic equilibrium with the ambient water (Fig. 3B). These results also suggest that the snapshot water data were not representative for the whole year at from Berria Beach.

Similarly, when the margin $\delta^{18}O_s$ values were converted into water temperatures using Eqs. (1) and (2), the results varied significantly depending on which $\delta^{18}O_w$ value is considered (−0.03 ‰ or +0.90 ‰). When using a $\delta^{18}O_w$ value of −0.03 ‰, the annual average SST ranged between 8.6 °C and 16.2 °C, with an average underestimation of 3.5°C with respect to the instrumental record (RMSE = 3.7 °C). With $\delta^{18}O_w$ = +0.90 ‰, the reconstructed temperatures ranged between 12.4 °C and 20.4 °C, with an average offset of 1.2 °C from measured SST (RMSE = 0.2 °C; Fig. 4).

Based on these results, further temperature reconstructions using the sequentially micromilled shells at Berria Beach were calculated using a $\delta^{18}O_w$ value of +0.90 ‰. The water temperature estimated from shells collected at the low-intertidal zone ranged between 12.6 ± 1.0 °C and 21.3 ± 1.3 °C (Table 4). The reconstructions based on the shells from the high intertidal zone show almost identical ranges (from 12.7 ± 0.2 °C to 21.5 ± 1.4 °C; Table 4).

4.3 Shell carbon isotopes

The ventral margins of shells from Berria Beach showed $\delta^{13}C_s$ values between −1.79 ‰ and −0.29 ‰, with higher values recorded during summer and autumn (Table 3). The correlations between $\delta^{13}C_s$, salinity and $\delta^{13}C_{DIC}$ were rather low (R= 0.10 and R= −0.15, n= 21, respectively). However, annual variances of $\delta^{13}C_s$ and SST were better correlated (R= 0.65, n= 21). The Berria Beach shells sampled sequentially showed similar ranges, with average annual $\delta^{13}C_s$ values of −0.50 ± 0.14 ‰ and −0.38 ± 0.23 ‰ (low and high intertidal zone, respectively; Table 4). The shells from Montehano and Carasa, instead, were characterised by lower $\delta^{13}C_s$ values (average of −1.02 ± 0.33 ‰ and −3.62 ± 0.59 ‰, Table 4).

4.4 Shell oxygen and carbon isotope correlations

The correlation between $\delta^{18}O_s$ and $\delta^{13}C_s$ varied among the different study localities (Fig. 5 and SI_1). Generally, negative relationships were visible in the marine habitat. For instance, the ventral margins of shells from Berria Beach had lower $\delta^{18}O_s$ during the warm season, whereas $\delta^{13}C_s$ were higher (Table 3). Similarly, the shells sampled sequentially showed the same pattern (Fig. 5A; SI_1). However, at Montehano and Carasa, the correlation was positive (Fig. 5B-C; SI_1). As a result, both Pearson coefficient (r) and correlation slopes were influenced by the geographical

gradient (Table 5; Fig. 6). The F-test was run to test the equality of the regression slopes and the results indicated that the slopes were statistically different from each other ($p < 0.01$).

5. Discussion

5.1 Water chemical properties

At Berria Beach, the salinity data indicated fully marine conditions. Similar values were recorded among the monthly collections from Langre Beach (Gutiérrez-Zugasti et al., 2017). The measured salinity range throughout the year was extremely narrow (ca 2 PSU), suggesting that even though the precipitation-evaporation cycle may induce a small degree of variance, no other freshwater inputs (i.e., river discharge) significantly affected the area. The uniform salinity challenged the interpretation of the observed $\delta^{18}O_w$ values. In temperate marine environments, $\delta^{18}O_w$ is generally characterised by higher values (between ca 0.80 ‰ and 2.00 ‰) (Schmidt et al., 1999; Prendergast and Schöne, 2017; Purroy et al., 2018). And, especially when considering areas with similar environmental conditions (i.e., Langre Beach; Gutiérrez-Zugasti et al., 2017), it becomes evident that the average $\delta^{18}O_w = -0.03$ ‰ largely deviates from the range of expected values. Considering that the oxygen isotope value in seawater is mainly influenced by hydrological processes such as evaporation, freshwater runoff and temperature (Garlick, 1974; Hoefs, 1997), at first sight, negative values observed at Berria Beach could be attributed to a constant freshwater input. However, this was not reflected in the measured salinity data and therefore, we can only hypothesize the possibility of unidentified factors inducing particularly low $\delta^{18}O_w$ values. For instance, potential groundwater influxes could be registered by the benthic organisms which are in

close contact with such waters, but the amounts would be so small that they would not affect the salinity of the water that has been sampled for measurements. Furthermore, instrumental failures can be excluded because that would cause erroneous output in specific samples and not throughout the dataset, like in this case.

A gradient towards lower $\delta^{18}O_w$ values was observed in the estuarine localities. This pattern depends on the fact that these two areas are strongly influenced by riverine influx, which in turn, due to the Rayleigh fractionation processes, is characterized by lower values than seawater (Gat, 1980). Particularly low $\delta^{18}O_w$ values were recorded at Carasa during autumn and winter. A similar geographical gradient was also visible for $\delta^{13}C_{DIC}$. In coastal environments, one of the major sources of carbon is the terrestrial biosphere, which in turn, due to photosynthetic pathways, is generally a reservoir of ^{13}C-depleted carbon (Mook and Vogel, 1968; O'Leary, 1981). As a result, the riverine carbon content is characterized by low $\delta^{13}C_{DIC}$ values, and it gradually increases toward the coastal areas due to water mass mixing. For this reason, $\delta^{13}C_{DIC}$ is strongly linked to salinity (Spiker, 1980; Fry, 2002). At all three study localities, the cold months were characterised by lower $\delta^{13}C_{DIC}$ values than the warm months. This coincided with the periods of higher precipitation and higher river runoff and therefore influx of ^{13}C-depleted DIC. Furthermore, during autumn and winter respiration by phytoplankton prevails over primary production, leading to a decrease of $\delta^{13}C_{DIC}$ (Quay et al., 1986; Sherr, 1982). On the contrary, during spring and summer, when photosynthesis dominates, there is an enrichment of ^{13}C in the DIC pool.

5.2 M. galloprovincialis shell deposition

The results obtained from the isotope analyses on the ventral margins from Berria Beach shells indicate that the shells were deposited near isotopic equilibrium with the surrounding water. The

predicted and measured $\delta^{18}O_s$ values showed similar sinusoidal trends although an average offset of 0.25 ± 0.17 ‰ was observed. Likewise, a previous study reported offsets from expected equilibrium in *Mytilus californianus*, ranging between 0.20 and 0.50 ‰ (Ford et al., 2010). The offsets between predicted and measured $\delta^{18}O_s$, observed in several mollusc species, are likely related to the temporal variance of $\delta^{18}O_w$ and to the shell growth rate (Ford et al., 2010; Gutiérrez-Zugasti et al., 2017).

Throughout the year, the larger offsets between predicted and measured $\delta^{18}O_s$ were observed in November and December 2017 (last three collection events). This might suggest that the shell deposition rate slightly decreased in this period. Growth slowdowns have been previously observed in most mollusc species (e.g., Lutz, 1980; Ivany et al., 2003; Marali and Schöne, 2015). In numerous species, the major seasonal growth slowdowns occur during the cold months (Orton, 1926; Fenger et al., 2007; Chavaud et al., 2011). However, the timing and duration of the seasonal slowdown are highly species-specific and site-specific (Hallmann et al., 2011; Purroy et al., 2018). As for *Mytilus* spp., specimens from southern Argentina showed a decline in shell production in autumn and winter (Lobbia, 2012). Similarly, sclerochronological observations on *M. edulis* from Scotland showed that narrower growth increments forming in this period (Richardson et al., 1990). Likewise, *M. galloprovincialis* from Tokyo Bay presented the same trend (Okaniwa et al., 2010)

Similar to the ventral margins, the micromilled *M. galloprovincialis* from Berria Beach did not show abrupt isotope shifts. This suggests that, even though shell deposition rate may be subjected to a decrease in late autumn, a major or prolonged cessation did not occur and shell was produced nearly year-round. As a result, the shells lacked well-defined annual growth lines, generally developed in other mytiloid species (e.g., Craig and Hallam 1963; Richardson et al. 1990). Furthermore, the larger offsets between predicted and measured $\delta^{18}O_s$ in November and December

2017 may also be related to a growth slowdown possibly related to the exceptionally intense rainfall and low temperature registered during these months.

5.3 Temperature reconstruction

Temperatures estimated from $\delta^{18}O_s$ (using $\delta^{18}O_w$ = +0.90 ‰) compared well to instrumental data. As mentioned in the previous section, the largest offset (2.5 °C) between measured and reconstructed temperature was recorded in late autumn. This was likely due to a slowdown of shell growth and has to be taken into account when using *M. galloprovincialis* for palaeoenvironmental reconstructions. However, the overall agreement between the measured and reconstructed temperatures supports the use of *M. galloprovincialis* as palaeothermometer as previously observed by Killingley and Berger (1979).

Furthermore, the results showed that the temperature reconstructions based on shells living in the high intertidal zone agree extremely well with the results from the low intertidal zone mussels. It is well known that shell deposition in intertidal species occurs when the animals are submerged (Clark, 1974; Ohno, 1982; Lønne and Gray, 1988). For this reason, differences in the submersion time may bias their respective geochemical signatures. However, the present results indicated that the submersion patterns were not significantly different to induce variations in the $\delta^{18}O_s$ and temperature reconstructions. It must be noted that the two collection sites were ca. 150 m apart. The collection spot in the lower intertidal was located just below the mean tide level, while the collection spot in the higher intertidal was situated between the mean tide level and the mean high water. Given that Berria Beach has a rather flat slope, the distance between collection spots translates into a minimum difference in the water submersion times of the mussels.

5.4 Shell carbon isotopes and provenance identification

Unlike $\delta^{18}O_s$, shell carbon isotope signature is not well understood (e.g., Lorrain et al., 2004; McConnaughey and Gillikin, 2008). It is acknowledged that the $\delta^{13}C_s$ derives from the incorporation of carbon from two main sources: the ambient inorganic carbon (water DIC) and the organic carbon assimilated through diet (Tanaka et al., 1986; McConnaughey et al., 1997; McConnaughey and Gillikin, 2008). Although it has been determined that the contribution of metabolic carbon is rather limited (10% or less), it is still challenging to establish a robust environmental proxy using $\delta^{13}C_s$ (McConnaughey et al., 1997; Lorrain et al., 2004; Gillikin et al., 2006). Our results indicated the existence of a geographical gradient among the three sites considered. As for the $\delta^{13}C_{DIC}$, the $\delta^{13}C_s$ values of the shells from estuarine localities were lower than the values of the marine specimens. Similar observations were previously made on *M. edulis* from an estuarine habitat by Gillikin et al. (2006). These authors concluded that $\delta^{13}C_s$ cannot be used to precisely reconstruct $\delta^{13}C_{DIC}$ due to the presence of metabolic carbon. However, it can provide an indication of salinity at large scale (i.e., with salinities differing by at least 5 PSU; Gillikin et al., 2006).

One of the aims of this study was to test whether the combination of oxygen and carbon isotope signatures can provide a reliable proxy for provenance. Our results showed that in marine settings (Berria Beach), $\delta^{18}O_s$ and $\delta^{13}C_s$ were negatively correlated. For instance, low $\delta^{13}C_s$ values occurred when $\delta^{18}O_s$ values were high, namely during the cold months. This is due to the fact that precipitationwas higher during autumn and winter. Likewise, evaporation was reduced and more ^{13}C-depleted DIC was received from terrestrial habitats. However, in estuarine habitats, the correlation between $\delta^{18}O_s$ and $\delta^{13}C_s$ was positive. The direction of the correlation may thus serve as a provenance indicator at the local scale. Previous studies on estuarine shells have shown similar

positive correlations between $\delta^{18}O_s$ and $\delta^{13}C_s$ (Khim et al., 2003; Gillikin et al., 2005; Verdegaal et al., 2005).

In order to better understand the mechanisms behind these different geochemical signals, it is important to consider the circumstances occurring at the time of deposition. This implies a direct comparison between water and shell chemistry. Besides the ventral margins that offer the most reliable calendar assignment, the oxygen isotope data of the micromilled specimens from Berria Beach can be used to place the shell portions in temporal context (i.e. summer/winter) based on the reconstructed temperature variations. The $\delta^{18}O_s$ data from the three different localities showed a similar pattern in the last shell portion formed before collection. All shells showed a gradual shift of $\delta^{18}O_s$ toward higher values. Considering the shells were collected around the same date and they had rather similar isotopic profiles in terms of curve shape, similar growth patterns were assumed. Certainly, this assumption cannot be used for a precise dating but it can provide a rough estimate of the time when the last shell portion was deposited. In the Berria Beach specimens, the $\delta^{18}O_s$ shift of the ventral margin related to the autumn temperature decrease. At Montehano and Carasa, the larger variance of $\delta^{18}O_w$, could have influenced the $\delta^{18}O_s$ data. However, in autumn both localities were characterized by a decrease in $\delta^{18}O_w$, while the shells showed an increase in the $\delta^{18}O_s$ values. This indicated that, in estuarine habitats, shell oxygen isotopes mainly reflected changes in water temperature, not $\delta^{18}O_w$. This hypothesis was also supported by the fact that $\delta^{18}O_s$ values in the Montehano specimens were rather similar to the Berria Beach ones, especially during winter, with a tendency towards more negative values in summer. Nonetheless, given that the degree of influence of the individual variables (temperature and $\delta^{18}O_w$) is not known, accurate temperature reconstructions using estuarine mussels will not be possible.

435 In specimens from Berria Beach and Montehano, post-summer $\delta^{13}C_s$ showed a trend toward
436 lower values, corresponding to a decrease in $\delta^{13}C_{DIC}$. However, the opposite trend was found in
437 the shells from Carasa. These results indicate that the change in the correlation sign between $\delta^{18}O_s$
438 and $\delta^{13}C_s$ is mainly influenced by the differing $\delta^{13}C_s$ signals in marine and freshwater-influenced
439 habitats.

440 The main source of carbon in the shells is the ambient dissolved inorganic fraction. According
441 to the freshwater-marine mixing profiles, the concentration of DIC in water largely depends on
442 salinity variations. At low salinity, i.e. in estuarine environments, a significant decrease in DIC is
443 recorded (Fry, 2002). Furthermore, a $\delta^{13}C_{DIC}$ gradient towards more negative values occurs with
444 decreasing salinities (Gillikin et al., 2006). The lower availability of DIC and its lower isotopic
445 composition likely influence mollusc $\delta^{13}C_s$ signatures and it may explain the observed differences
446 between marine and estuarine specimens. Furthermore, mussels are highly selective feeders and
447 they tend to assimilate a minor amount of carbon from the phytoplankton they ingest (Gillikin et
448 al., 2005). In turn, the fractionation between phytoplankton and DIC can largely be influenced by
449 water DIC concentrations, light levels and kinetics effects related to specific metabolic pathways
450 of different phytoplankton species (O'Leary, 1981; Farquhar et al., 1982; Rau et al., 1982; Popp et
451 al., 1998). Coastal and estuarine habitats are characterised by strong environmental gradients of
452 physical and chemical variables, which significantly influence the diversity of the phytoplankton
453 communities. For instance, a study conducted on the River Pas estuary (ca 40 km west to localities
454 studied here) revealed that areas at the river mouth show elevated phytoplankton productivity and
455 diversity, but low biomass, whereas more interior localities reveal the opposite (Pérez and
456 Canteras, 1990). Therefore, the different plankton communities among marine, estuarine and
457 freshwater habitats may have an important influence on the carbon uptake and fractionation

processes resulting in different plankton $\delta^{13}C$ values available for the mussels. Further studies are needed to better understand the geographical variation of plankton $\delta^{13}C$ in connection with estuarine environments and its importance in the mollusc $\delta^{13}C_s$ signature. However, our preliminary results suggested that the direction, and therefore the slope of the correlation between $\delta^{18}O_s$ and $\delta^{13}C_s$ may be used as an indicator of *M. galloprovincialis* shell provenance, especially between marine and upper estuarine environments. The similarity of the correlation between the two shell isotope values found in marine and lower estuarine habitats may lead to a challenging provenance determination within these two areas. In this case, the more negative $\delta^{13}C_s$ and $\delta^{18}O_s$ (especially in summer) values recorded in the low estuarine shells, compared to the marine shells, may be used for further clarification.

6. Conclusions

This calibration study tested the suitability of *M. galloprovincialis* shells as a palaeotemperature archive. Results indicated that the mussels collected from the marine environment recorded the full seasonal temperature range in form of $\delta^{18}O_s$. The water temperature could be reconstructed with an average offset of 1.2 ± 0.7 °C with respect to measured SST, supporting the use of this species for palaeoenvironmental reconstructions as well as for determining shellfish collection seasonality in archaeological shell midden studies.

Furthermore, the present study investigated the geochemical signature of the shell in relation to the provenance of the mussels. The data from specimens collected in marine and estuarine habitats showed different correlations between $\delta^{18}O_s$ and $\delta^{13}C_s$. The negative correlations characterising the marine specimens gradually increased following the geographical gradient from the coastal area to

481 the estuary. Therefore, the slope of such correlations is suggested to be a potential indicator to
482 identify the type of habitat in which the molluscs lived. This information, in turn, could be applied
483 to archaeological studies to spatially analyse collection preferences of human societies relying on
484 shellfish exploitation as food and raw material resource. Furthermore, the ability to recognise
485 estuarine shells can represent an important tool allowing to discard these specimens from further
486 palaeoenvironmental analyses and avoid potential erroneous water temperature reconstructions.
487
488

489 Acknowledgements

490 This research was performed as part of the projects HAR2016-75605-R and HAR2017-86262-P,
491 funded by the Spanish Ministry of Economy and Competitiveness, MINECO. We thank the
492 Fishing Activity Service of the Cantabrian Government and the Natural Park of the Santoña
493 Marshlands for the authorization to collect modern mussels, and the SeaDataNet Pan-European
494 infrastructure for ocean and marine data management (http://www.seadatanet.org) for providing
495 current seawater temperatures in the region. We also thank to the Max Planck Institute for
496 Evolutionary Anthropology, University of Mainz, Universidad de Cantabria (UC) and Instituto
497 Internacional de Investigaciones Prehistóricas de Cantabria (IIIPC), for providing support. We
498 would also like to thank José Ramón Mira Soto (UC) for measuring the salinity and Lucía Agudo
499 Pérez (IIIPC) for helping with the shell collection and post-collection processes.
500
501

502 References

503 Abada-Boudjema YM and Dauvin JC (1995) Recruitment and life span of two natural mussel
504 populations *Perna perna* (Linnaeus) and *Mytilus galloprovincialis* (Lamarck) from the
505 algerian coast. *Journal of Molluscan Studies* 61(4): 467–481. DOI: 10.1093/mollus/61.4.467.

506 Álvarez I, Gomez-Gesteira M, DeCastro M, et al. (2010) Summer upwelling frequency along the
507 western Cantabrian coast from 1967 to 2007. *Journal of Marine Systems* 79(1–2). Elsevier
508 B.V.: 218–226. DOI: 10.1016/j.jmarsys.2009.09.004.

509 Alvarez I, Gomez-Gesteira M, deCastro M, et al. (2011) Comparative analysis of upwelling
510 influence between the western and northern coast of the Iberian Peninsula. *Continental Shelf*
511 *Research* 31(5). Elsevier: 388–399. DOI: 10.1016/j.csr.2010.07.009.

512 Barsotti G, Meluzzi C (1968). Osservazioni su *Mytilus edulis* L. e *Mytilus galloprovincialis*
513 Lamarck. *Conchiglie* 4: 50 –58.

514 Botas JA, Fernandez E, Bode A, et al. (1989) Water masses off the Central Cantabrian Coast.
515 *Scientia Marina* 53: 755–761.

516 Burchell M, Cannon A, Hallmann N, et al. (2013) Refining estimates for the season of shellfish
517 collection on the Pacific Northwest coast: Applying high-resolution stable oxygen isotope
518 analysis and sclerochronology. *Archaeometry* 55(2): 258–276. DOI: 10.1111/j.1475-
519 4754.2012.00684.x.

520 Chauvaud L, Thébault J, Clavier J, et al. (2011) What's hiding behind ontogenetic $\delta^{13}C$ variations
521 in mollusk shells? New insights from the great scallop (*Pecten maximus*). *Estuaries and*
522 *Coasts* 34(2): 211–220. DOI: 10.1007/s12237-010-9267-4.

523 Clark GRI (1974) Calcification on an Unstable Substrate : Marginal Growth in the Mollusk Pecten
524 diegensis. *Science* 183: 968–970.

525 Craig GY and Hallam A (1963) Size-frequency and growth-ring analyses of *Mytilus edulis* and
526 *Cardium edule*, and their palaeoecological significance. *Palaeontology* 6: 731–750.

527 Diz AP and Presa P (2009) The genetic diversity pattern of *Mytilus galloprovincialis* in Galician
528 Rías (NW Iberian estuaries). *Aquaculture* 287(3–4). Elsevier B.V.: 278–285. DOI:
529 10.1016/j.aquaculture.2008.10.029.

530 Epstein S, Buchsbaum R, Lowenstam HM, et al. (1953) Revised carbonate-water isotopic
531 temperature scale. *Bulletin of the Geological Society of America* 64: 1315–1326.

532 Farquhar GD, O'Leary MH and Berry JA (1982) On the relationship between carbon isotope
533 discrimination and the intercellular carbon dioxide concentration in leaves. *Australian*
534 *Journal of Plant Physiology* 9: 121–137.

535 Feng QL, Li HB, Pu G, et al. (2000) Crystallographic alignment of calcite prisms in the oblique
536 prismatic layer of *Mytilus edulis* shell. *Journal of Materials Science* 35(13): 3337–3340. DOI:
537 10.1023/A:1004843900161.

538 Fenger T, Surge D, Schöne B, et al. (2007) Sclerochronology and geochemical variation in limpet
539 shells (*Patella vulgata*): A new archive to reconstruct coastal sea surface temperature.
540 *Geochemistry, Geophysics, Geosystems* 8(7). DOI: 10.1029/2006GC001488.

541 Flores C, Figueroa V and Salazar D (2016) Middle Holocene Production of Mussel Shell Fishing
542 Artifacts on the Coast of Taltal (25° Lat South), Atacama Desert, Chile. *Journal of Island and*
543 *Coastal Archaeology* 11(3): 411–424. DOI: 10.1080/15564894.2015.1105884.

544 Ford HL, Schellenberg SA, Becker BJ, et al. (2010) Evaluating the skeletal chemistry of *Mytilus*
545 *californianus* as a temperature proxy: Effects of microenvironment and ontogeny.
546 *Paleoceanography* 25(1). DOI: 10.1029/2008PA001677.

547 Friedman I and O'Neil JR (1977) Compilation of stable isotope fractionation factors of
548 geochemical interest. In: Fleischer M (ed.) *Data of Geochemistry*. Washington, DC: United
549 States Department of Interior, pp. 1–12. DOI: 10.1016/S0016-0032(20)90415-5.

550 Fry B (2002) Conservative mixing of stable isotopes across estuarine salinity gradients: A
551 conceptual framework for monitoring watershed influences on downstream fisheries
552 production. *Estuaries* 25: 264–271.

553 Füllenbach CS, Schöne BR and Mertz-Kraus R (2015) Strontium/lithium ratio in aragonitic shells
554 of *Cerastoderma edule* (Bivalvia) - A new potential temperature proxy for brackish
555 environments. *Chemical Geology* 417. Elsevier B.V.: 341–355. DOI:
556 10.1016/j.chemgeo.2015.10.030.

557 Garlick GD (1974) The stable isotopes of oxygen, carbon, hydrogen in the marine environment.
558 In: Goldberg ED (ed.) *The Sea, vol. 5*, pp. 393–425.
559
560 Gat JR (1980) The isotopes of hydrogen and oxygen in precipitation. In: Fritz P and Fontes J (eds)
561 *Handbook of Environmental Isotope Geochemistry Vol. 1, The Terrestrial Environment,*
562 Amsterdam: Elesevier, pp. 21–48

563 Gillikin DP, De Ridder F, Ulens H, et al. (2005) Assessing the reproducibility and reliability of
564 estuarine bivalve shells (*Saxidomus giganteus*) for sea surface temperature reconstruction:
565 Implications for paleoclimate studies. *Palaeogeography, Palaeoclimatology, Palaeoecology*
566 228(1–2): 70–85. DOI: 10.1016/j.palaeo.2005.03.047.

567 Gillikin DP, Lorrain A, Bouillon S, et al. (2006) Stable carbon isotopic composition of *Mytilus*
568 *edulis* shells: relation to metabolism, salinity, $d^{13}C$ DIC and phytoplankton. *Organic*
569 *Geochemistry* 37(10): 1371–1382. DOI: 10.1016/j.orggeochem.2006.03.008.

570 Grossman EL and Ku T (1986) Oxygen and carbon isotope fractionation in biogenic aragonite:
571 Temperature effects. *Chemical Geology* 59: 59–74.

572 Gutiérrez-Zugasti I, Garcia-Escarzaga A, Martin-Chivelet J, et al. (2015) Determination of sea
573 surface temperatures using oxygen isotope ratios from *Phorcus lineatus* (Da Costa, 1778) in
574 northern Spain: Implications for paleoclimate and archaeological studies. *The Holocene* 25:
575 1002–1014. DOI: 10.1177/0959683615574892.

576 Gutiérrez-Zugasti I, Suárez-Revilla R, Clarke LJ, et al. (2017) Shell oxygen isotope values and
577 sclerochronology of the limpet *Patella vulgata* Linnaeus 1758 from northern Iberia:
578 Implications for the reconstruction of past seawater temperatures. *Palaeogeography,*
579 *Palaeoclimatology, Palaeoecology* 475. Elsevier B.V.: 162–175. DOI:
580 10.1016/j.palaeo.2017.03.018.

581 Hallmann N, Schöne BR, Irvine GV, et al. (2011) An improved understanding of the Alaska coastal
582 current: the application of a bivalve growth-temperature model to reconstruct freshwater-
583 influenced paleoenvironments. *Palaios* 26(6): 346–363. DOI: 10.2110/palo.2010.p10-151r.

584 Hallmann N, Burchell M, Schöne BR, et al. (2009) High-resolution sclerochronological analysis
585 of the bivalve mollusk *Saxidomus gigantea* from Alaska and British Columbia: techniques
586 for revealing environmental archives and archaeological seasonality. *Journal of*
587 *Archaeological Science* 36(10): 2353–2364. DOI: 10.1016/j.jas.2009.06.018.

588 Hilbish TJ, Mullinax A, Dolven SI, et al. (2000) Origin of the antitropical distribution pattern in
589 marine mussels (*Mytilus* spp.): routes and timing of transequatorial migration. *Marine Biology*
590 136: 69–77. DOI: 10.1007/s12031-012-9836-z.

591 Hoefs J (1997) *Stable Isotope Geochemistry*. Berlin: Springer-Verlag.

592 Ivany LC, Wilkinson BH and Jones DS (2003) Using stable isotopic data to resolve rate and
593 duration of growth throughout ontogeny: An example from the surf clam, *Spisula solidissima*.
594 *Palaios* 18(2): 126–137. DOI: 10.1669/0883-1351(2003)18<126:USIDTR>2.0.CO;2.

595 Jones DS (1983) Sclerochronology: reading the record of the molluscan shell. *American Scientist*
596 71(4): 384–391.

597 Khim B-K, Krantz DE, Cooper LW, et al. (2003) Seasonal discharge of estuarine freshwater to the
598 western Chukchi Sea shelf identified in stable isotope profiles of mollusk shells. *Journal of*
599 *Geophysical Research* 108(C9): 3300. DOI: 10.1029/2003JC001816.

600 Killingley JS and Berger WH (1979) Stable isotopes in a mollusk shell: detection of upwelling
601 events. *Science* 205: 186–188. DOI: 10.1126/science.205.4402.186.

Lobbia PA (2012) Esclerocronología en valvas de Mytilus spp: Analisis del sitio CCH4 (Parque Nacional Monte Leon, Santa Cruz, Argentina) e implicaciones para la arqueologia de Patagonia. *Magallania* 40: 221–231.

Lønne OJ and Gray JS (1988) Influence of tides on migrogrowth bands in *Cerastoderma edule* from Norway. *Marine Ecology Progress Series* 42: 1–7.

Lorrain A, Paulet YM, Chauvaud L, et al. (2004) δ13C variation in scallop shells: Increasing metabolic carbon contribution with body size? *Geochimica et Cosmochimica Acta* 68(17): 3509–3519. DOI: 10.1016/j.gca.2004.01.025.

Lutz RA (1976) Annual growth patterns in the inner shell layer of *Mytilus edulis* L. *Journal of the Marine Biological Association of the United Kingdom* 56(3): 723–731. DOI: 10.1017/S0025315400020750.

Lutz, RA (1980). Growth patterns within the molluscan shell: an overview. *Skeletal Growth of Aquatic Organisms: Biological Records of Environmental Change (Topics in Geobiology)*, 203-254.

Maire O, Amouroux JM, Duchêne JC, et al. (2007) Relationship between filtration activity and food availability in the Mediterranean mussel *Mytilus galloprovincialis*. *Marine Biology* 152(6): 1293–1307. DOI: 10.1007/s00227-007-0778-x.

Mannino MA, Thomas KD, Leng MJ, et al. (2007) Marine resources in the mesolithic and neolithic at the Grotta dell'Uzzo (Sicily): Evidence from isotope analyses of marine shells. *Archaeometry* 49: 117–133. DOI: 10.1111/j.1475-4754.2007.00291.x.

Marali S and Schöne BR (2015) Oceanographic control on shell growth of *Arctica islandica* (Bivalvia) in surface waters of Northeast Iceland - Implications for paleoclimate reconstructions. *Palaeogeography, Palaeoclimatology, Palaeoecology* 420. 138–149. DOI: 10.1016/j.palaeo.2014.12.016.

Marchitto TM, Jones GA, Goodfriend GA, et al. (2000) Precise temporal correlation of Holocene mollusk shells using sclerochronology. *Quaternary Research* 53: 236–246. DOI: 10.1006/qres.1999.2107.

Marean CW, Bar-Matthews M, Bernatchez JA, et al. (2007) Early human use of marine resources and pigment in South Africa during the Middle Pleistocene. *Nature* 449(October): 906–909. DOI: 10.1038/nature06204.

McConnaughey TA, Burdett J, Whelan JF, et al. (1997) Carbon isotopes in biological carbonates: Respiration and photosynthesis. *Geochimica et Cosmochimica Acta* 61: 611–622.

McConnaughey TA and Gillikin DP (2008) Carbon isotopes in mollusk shell carbonates. *Geo-Marine Letters* 28: 287–299. DOI: 10.1007/s00367-008-0116-4.

McDonald JH and Koehn RK (1988) The mussels *Mytilus galloprovincialis* and *M. trossulus* on the Pacific coast of North America. *Marine Biology* 99(1): 111–118. DOI: 10.1007/BF00644984.

McDonald JH, Seed R and Koehn RK (1991) Allozymes and morphometric characters of three species of *Mytilus* in the Northern and Southern Hemispheres. *Marine Biology* 111: 323–333. DOI: 10.1038/053222a0.

Mook WG and Vogel JC (1968) Isotopic equilibrium between shells and their environment. *Nature* 159: 874–875. DOI: 10.1038/098448b0.

Ohno T (1982) A note on the variability of growth increment formation in the shell of the common cockle *Cerastoderma edule*. In: *Tidal Friction and the Earth's Rotation II*. Springer Berlin Heidelberg, pp. 222–228.

Okaniwa N, Miyaji T, Sasaki T, et al. (2010) Shell growth and reproductive cycle of the Mediterranean mussel *Mytilus galloprovincialis* in Tokyo Bay, Japan: relationship with environmental conditions. *Plankton and Benthos Research* 5: 214–220. DOI: 10.3800/pbr.5.214.

O'Leary MH (1981) Carbon isotope fractionation in plants. *Phytochemistry* 20(4): 553–567. DOI: 10.1016/0031-9422(81)85134-5.

Orton JH (1926) On the rate of growth of *Cardium edule*. Part I. Experimental observations. *Journal of the Marine Biological Association of the United Kingdom* 14(2): 239–279.

Peharda M, Župan I, Bavčević L, et al. (2007) Growth and condition index of mussel *Mytilus galloprovincialis* in experimental integrated aquaculture. *Aquaculture Research* 38(16): 1714–1720. DOI: 10.1111/j.1365-2109.2007.01840.x.

Pérez L and Canteras JC (1993) Phytoplankton photosynthsis-light relationship in the Pas estuary, Cantabria, Spain. *Limnetica* 9: 61–66. DOI: 10.1093/humrep/13.3.576.

Pérez L and Canteras JC (1990) Spatial heterogeneity of phytoplankton in an estuary of Cantabria, Northern Spain. *Journal of Coastal Research* 6(1): 157–168.

Popp BN, Laws EA, Bidigare RR, et al. (1998) Effect of phytoplankton cell geometry on carbon isotopic fractionation. *Geochimica et Cosmochimica Acta* 62: 69–77. DOI: 10.1095/biolreprod12.5.584.

Prego R, Boi P and Cobelo-García A (2008) The contribution of total suspended solids to the Bay of Biscay by Cantabrian Rivers (northern coast of the Iberian Peninsula). *Journal of Marine Systems* 72(1–4): 342–349. DOI: 10.1016/j.jmarsys.2007.01.011.

Prendergast AL and Schöne BR (2017) Oxygen isotopes from limpet shells: Implications for palaeothermometry and seasonal shellfish foraging studies in the Mediterranean.

670 *Palaeogeography, Palaeoclimatology, Palaeoecology* 484: 33–47. DOI:
671 10.1016/j.palaeo.2017.03.007.

672 Prendergast AL, Stevens RE, O'Connell TC, et al. (2016) Changing patterns of eastern
673 Mediterranean shellfish exploitation in the Late Glacial and Early Holocene : Oxygen isotope
674 evidence from gastropod in Epipaleolithic to Neolithic human occupation layers at the Haua
675 Fteah cave, Libya. *Quaternary International* 407: 80–93. DOI: 10.1016/j.quaint.2015.09.035.

676 Purroy A, Milano S, Schöne BR, et al. (2018) Drivers of shell growth of the bivalve, *Callista*
677 *chione* (L. 1758) - Combined environmental and biological factors. *Marine Environmental*
678 *Research* 134: 138–149. DOI: 10.1016/j.marenvres.2018.01.011.

679 Quay PD, Emerson SR, Quay BM, et al. (1986) The carbon cycle for Lake Washington-A stable
680 isotope study. *Limnology and Oceanography* 31: 596–611.

681 Rau GH, Sweeney RE and Kaplan IR (1982) Plankton ^{13}C:^{12}C ratio changes with latitude:
682 differences between northern and southern oceans. *Deep-Sea Research* 29: 1035–1039.

683 Richardson CA, Seed R and Naylor E (1990) Use of internal growth bands for measuring
684 individual and population growth rates in *Mytilus edulis* from offshore production platforms.
685 *Marine Ecology Progress Series* 66: 259–265. DOI: 10.3354/meps066259.

686 Richardson CA (1989) An analysis of the microgrowth bands in the shell of the common mussel
687 *Mytilus edulis*. *Journal of the Maine Biological Association UK* 69: 477–491.

688 Sanjuan A, Zapata C and Alvarez G (1997) Genetic differentiation in *Mytilus galloprovincialis*
689 Lmk. throughout the world. *Ophelia* 47(1): 13–31. DOI: 10.1080/00785326.1997.10433387.

690 Schmidt GA, Bigg GR, Rohling EJ (1999) *Global Seawater Oxygen-18 Database - v1.22*
691 https://data.giss.nasa.gov/o18data/

692 Schöne BR (2008) The curse of physiology—challenges and opportunities in the interpretation of
693 geochemical data from mollusk shells. *Geo-Marine Letters* 28: 269–285. DOI:
694 10.1007/s00367-008-0114-6.

695 Schöne BR, Freyre Castro AD, Fiebig J, et al. (2004) Sea surface water temperatures over the
696 period 1884–1983 reconstructed from oxygen isotope ratios of a bivalve mollusk shell
697 (*Arctica islandica*, southern North Sea). *Palaeogeography, Palaeoclimatology,*
698 *Palaeoecology* 212: 215–232. DOI: 10.1016/j.palaeo.2004.05.024.

699 Schöne BR and Gillikin DP (2013) Unraveling environmental histories from skeletal diaries —
700 Advances in sclerochronology. *Palaeogeography, Palaeoclimatology, Palaeoecology* 373.
701 Elsevier B.V.: 1–5. DOI: 10.1016/j.palaeo.2012.11.026.

702 Seed R (1992) Systematics, evolution and distribution of mussels belonging to the genus *Mytilus*:
703 an overview. American Malacological Bulletin 9:123–137.

Seed R, Suchanek TH (1992) Population and community ecology of *Mytilus*. *The mussel Mytilus: ecology, physiology, genetics and culture*, *25*:87–170.

Sherr EB (1982) Carbon isotope composition of organic seston and sediments in a Georgia salt marsh estuary. *Geochimica et Cosmochimica Acta* 46(7): 1227–1232. DOI: 10.1016/0016-7037(82)90007-2.

Soto M, Kortabitarte M and Marigomez I (1995) Bioavailable heavy metals in estuarine waters as assessed by metal/shell-weight indices in sentinel mussels *Mytilus galloprovincialis*. *Marine Ecology Progress Series* 125: 127–136. DOI: 10.3354/meps125127.

Spiker EC (1980) The Behavior of ^{14}C and ^{13}C in Estuarine Water: Effects of In Situ CO_2 Production and Atmospheric Exchange. *Radiocarbon* 22(3): 647–654.

Tanaka N, Monaghan MC and Rye DM (1986) Contribution of metabolic carbon to mollusc and barnacle shell carbonate. *Nature* 320(6062): 520–523. DOI: 10.1038/320520a0.

Taylor JD, Kennedy WJ, Hall A (1969) The shell structure and mineralogy of the bivalvia. *Bulletin of the British Museum* 3:1–125.

Vanhaeren M, d'Errico F (2005) Grave goods from the Saint-Germain-la-Rivière burial: Evidence for social inequality in the Upper Palaeolithic. *Journal of Anthropological Archaeology* 24: 117-134.

Verdegaal S, Troelstra SR, Beets CJ, et al. (2005) Stable isotopic records in unionid shells as a paleoenvironmental tool. *Geologie en Mijnbouw/Netherlands Journal of Geosciences* 84(4): 403–408. DOI: 10.1017/S0016774600021211.

Villalba A (1995) Gametogenic cycle of cultured mussel, *Mytilus galloprovincialis*, in the bays of Galicia (N.W. Spain). *Aquaculture* 130: 269–277. DOI: 10.1016/0044-8486(94)00213-8.

Waite JH (1992) The formation of mussel byssus: anatomy of a natural manufacturing process. In: Case ST (ed) *Results and problems in cell differentiation, vol 19.* Berlin Heidelberg: Springer, pp 27–54.

Figures and tables

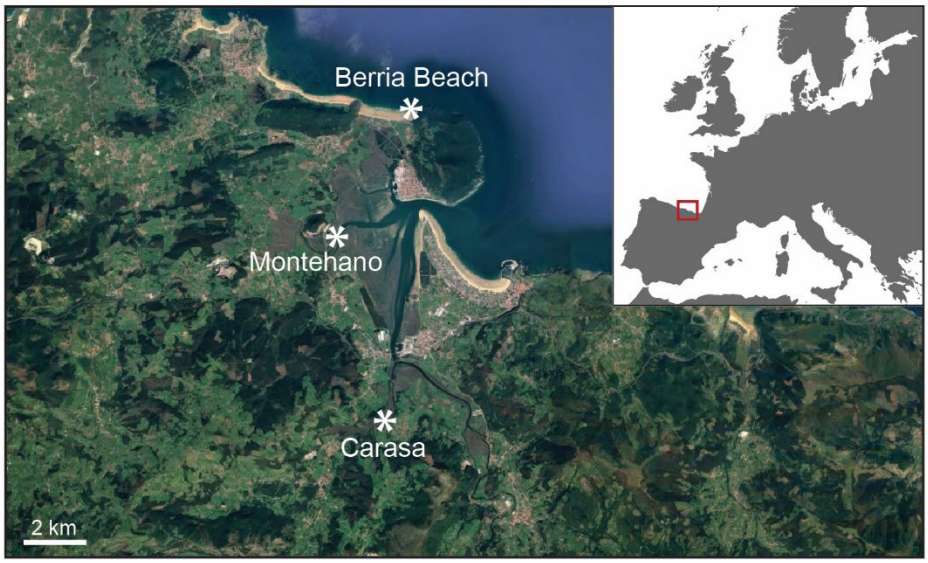

Fig. 1 Map of the three localities analysed in this study: Berria Beach (marine habitat), Montehano (lower estuarine habitat) and Carasa (upper estuarine habitat).

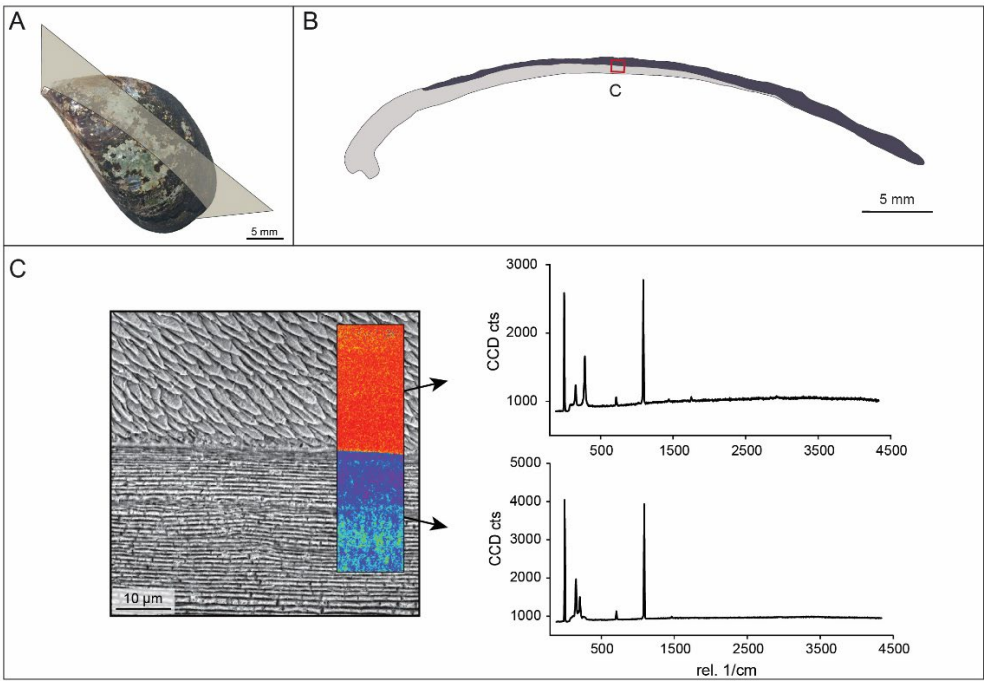

743

744 **Fig. 2** Structure and composition of *M. galloprovincialis* shell. (A) Shell overview with grey plane
745 indicating how the shell was sectioned (axis of maximum growth). (B) Sketch of the section
746 showing the shell subdivision in two layers. The light grey area represents the aragonitic layer and
747 the dark grey area represents the calcitic portion. (C) Scanning Electron Microscope image of the
748 prismatic and nacre layers and their respective Raman spectra. The Raman scan identifies the two
749 different $CaCO_3$ polymorphs based on the presence or absence of the aragonite librational peak L_a
750 at 206 cm^{-1}.

751

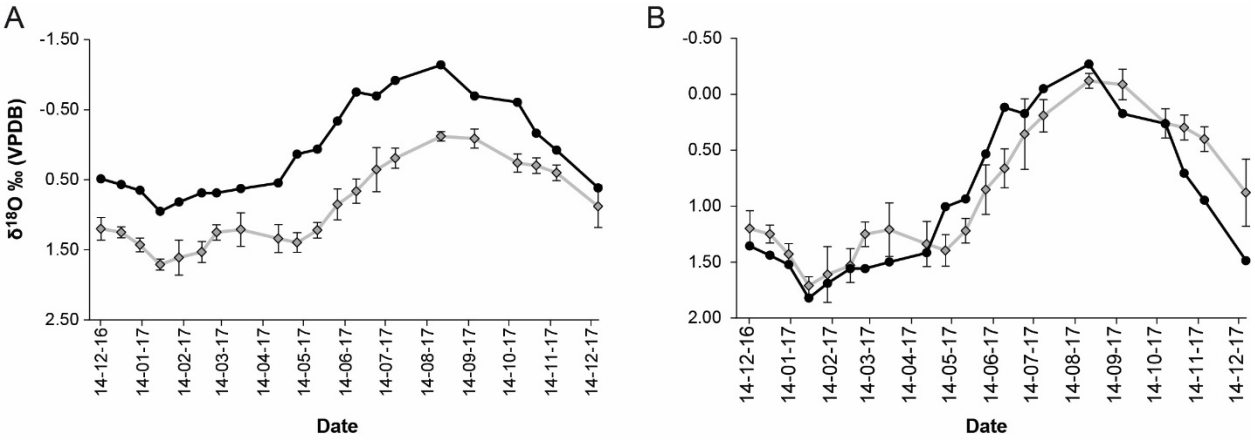

752

753 **Fig. 3** Measured (grey diamonds) and predicted (black circles) $\delta^{18}O_s$ values of the ventral margins
754 collected on bi-monthly basis (every two weeks) from Berria Beach. (A) Predicted $\delta^{18}O_s$ values
755 using $\delta^{18}O_w = -0.03$ ‰ in Eq. (2). (B) Predicted $\delta^{18}O_s$ values using $\delta^{18}O_w = +0.90$ ‰ in Eq. (2).

756

757

758

759

760

761

762

763

764

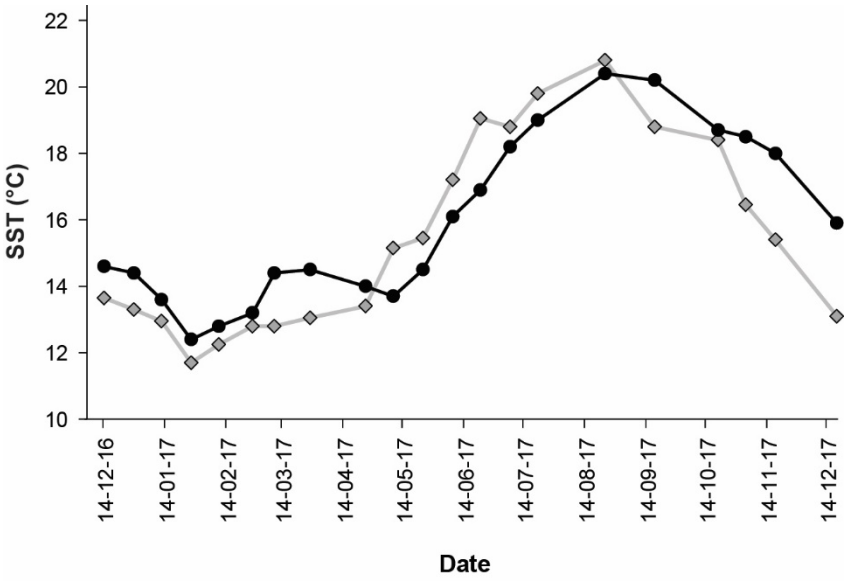

765

766 **Fig. 4** Water temperature reconstruction (black circles) using the $\delta^{18}O_s$ of the Berria Beach ventral
767 margins and $\delta^{18}O_w = +0.90$ ‰ in Eq. (2). The grey diamonds represent the measured SST at the
768 site.

769

770

771

772

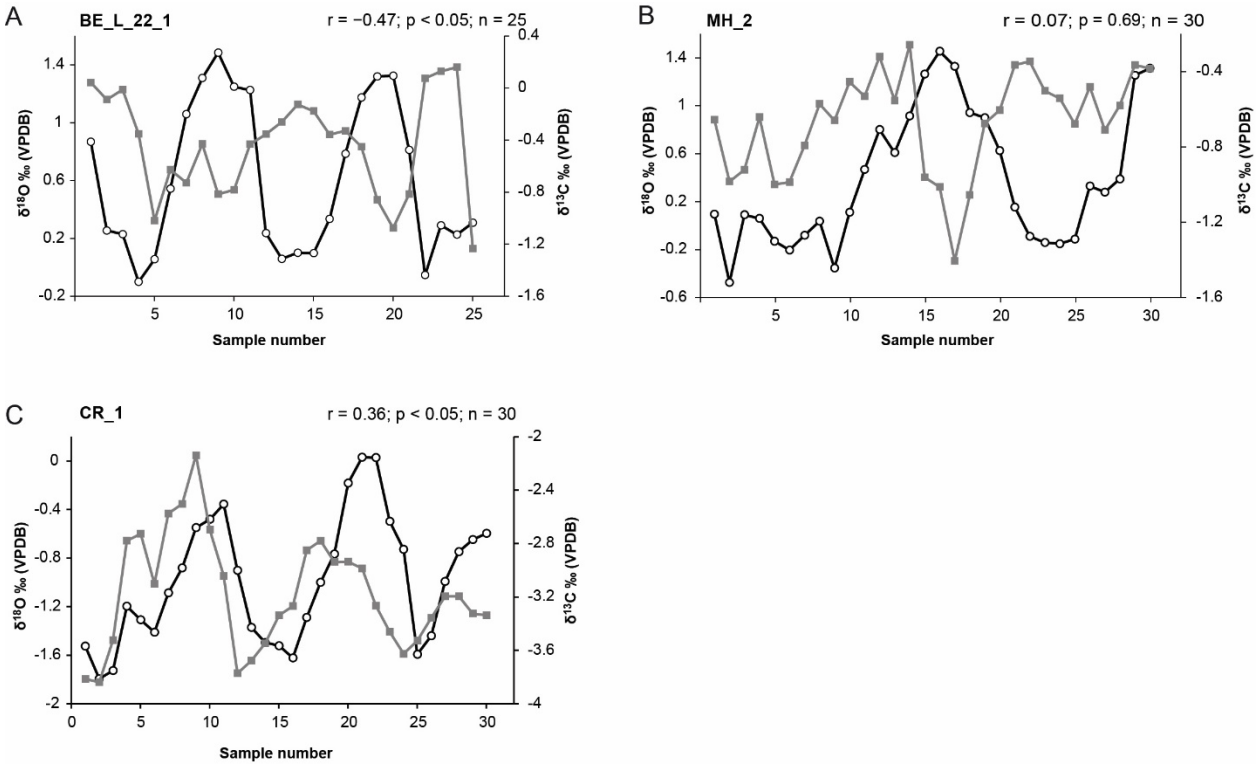

773

774 **Fig. 5** Examples of sequential $\delta^{18}O_s$ (open circles) and $\delta^{13}C_s$ results (grey squares and secondary y-
775 axes) of specimens from (A) Berria Beach (BE_L_22_1), (B) Montehano (MH_2) and (C) Carasa
776 (CR_1). The last data points in each graph represent the ventral margins. The isotope profiles of
777 the remaining micromilled shells can be found in the supplements (SI_1).

778

779

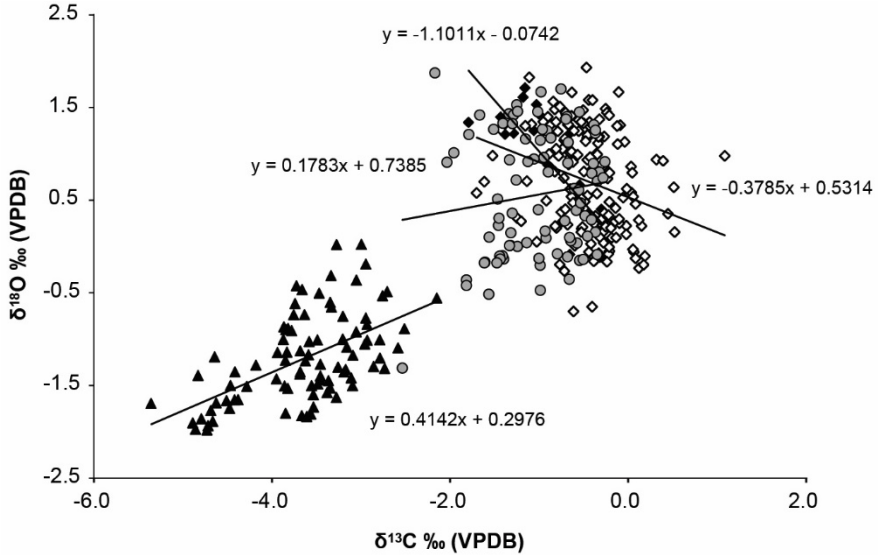

780

781 **Fig. 6** Linear relationships between $\delta^{13}C_s$ and $\delta^{18}O_s$ obtained from the ventral margins of shells
782 collected at Berria Beach (black diamonds), the micromilled shells from Berria Beach (open
783 diamonds), the shells from Montehano (grey circles) and the shells from Carasa (black triangles).

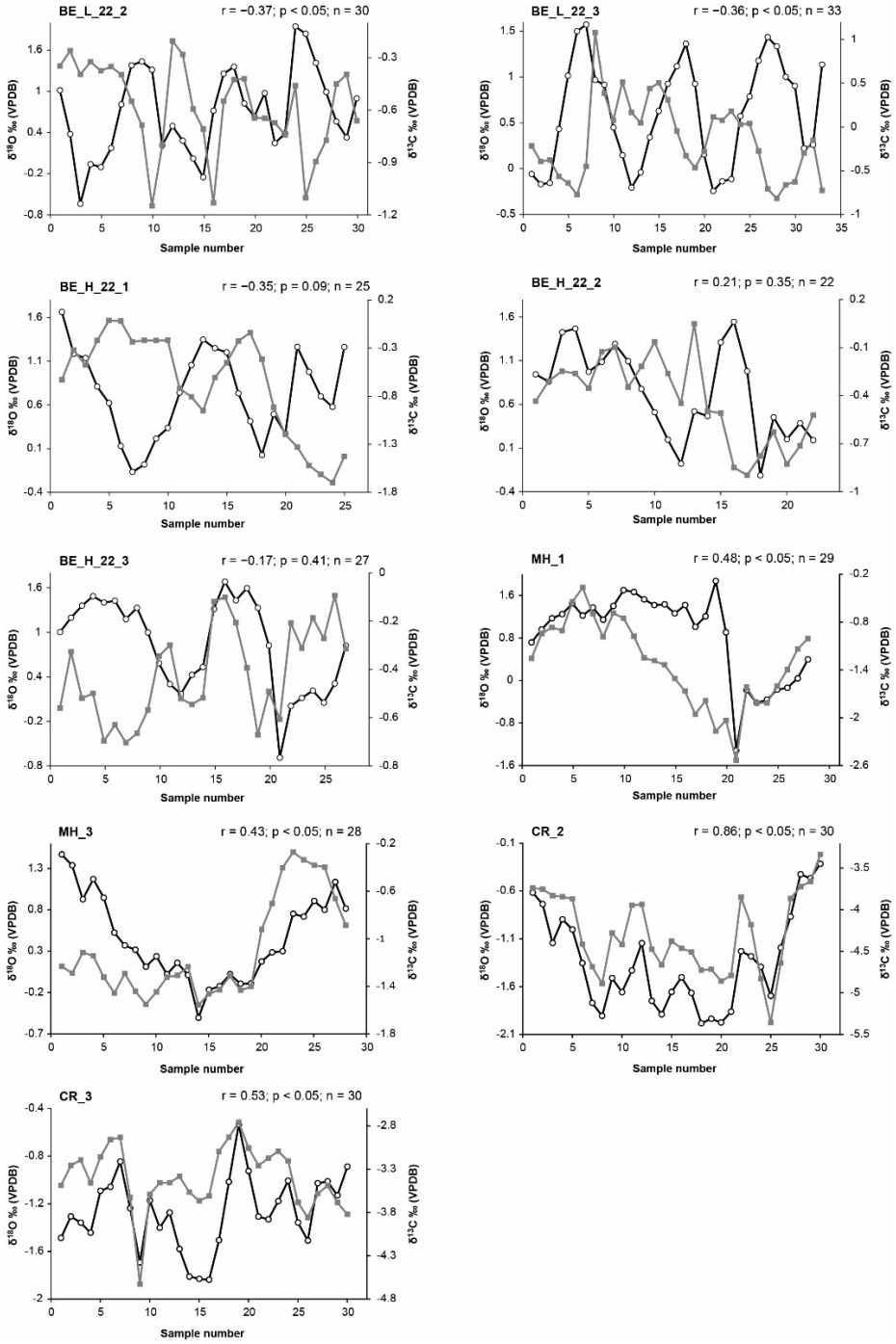

784

785 **Fig. SI_1**. Sequential $\delta^{18}O_s$ (open circles) and $\delta^{13}C_s$ profiles (grey squares and secondary y-axes)
786 of specimens from Berria Beach low intertidal (BE_L), Berria Beach high intertidal (BE_H),
787 Montehano (MH) and Carasa (CR). The last data points in each graph represent the ventral
788 margins.

Table 1. Seasonal water data recorded at the three locations considered in this study. In italics are the data that were potentially affected by temporary biases and therefore precluded from further analyses.

Berria Beach					Montehano					Carasa				
Date	Salinity (PSU)	SST (℃)	$\delta^{18}O_{VSMOW}$ (‰)	$\delta^{13}C_{VPDB}$ (‰)	Date	Salinity (PSU)	SST (℃)	$\delta^{18}O_{VSMOW}$ (‰)	$\delta^{13}C_{VPDB}$ (‰)	Date	Salinity (PSU)	SST (℃)	$\delta^{18}O_{VSMOW}$ (‰)	$\delta^{13}C_{VPDB}$ (‰)
14-12-16	35.3	13.7	-0.13	-3.73	14-12-16	35.3	14.1	0.28	-4.58	14-12-16	30.0	12.5	-0.80	-5.61
29-12-16	35.4	13.3	-0.07	-4.83	30-12-16	34.9	13.4	0.06	-3.79	30-12-16	26.1	11.9	-1.88	-6.64
12-01-17	35.3	13.0	-0.18	-5.59	12-01-17	33.5	13.0	-0.13	-4.35	12-01-17	1.7	11.9	-6.29	-11.66
27-01-17	35.6	11.7	-0.11	-4.96	27-01-17	34.2	11.2	-0.14	-4.06	27-01-17	27.1	10.0	-1.43	-5.48
10-02-17	35.7	12.3	-0.08	-5.18	09-02-17	28.7	11.9	-1.24	-5.22	09-02-17	6.9	10.9	-5.14	-10.03
27-02-17	35.8	12.8	-0.12	-4.38	28-02-17	35.4	13.2	0.16	-3.27	28-02-17	30.5	12.9	-0.72	-4.38
10-03-17	35.9	12.8	-0.04	-3.61	10-03-17	34.1	14.8	-0.21	-4.19	10-03-17	25.8	14.7	-1.80	-5.58
28-03-17	35.7	13.1	-0.10	-2.80	28-03-17	35.1	14.5	-0.13	-3.57	28-03-17	27.5	14.1	-1.39	-5.54
11-04-17	35.9	16.6	0.04	-3.65	11-04-17	34.6	16.6	-0.07	-3.88	11-04-17	28.0	16.8	-1.39	-5.50
25-04-17	35.9	13.4	-0.04	-3.11	25-04-17	35.2	14.7	0.19	-3.65	25-04-17	32.5	16.1	-0.26	-4.31
09-05-17	35.9	15.2	0.42	-3.25	09-05-17	34.7	16.0	0.00	-3.31	09-05-17	27.5	17.8	-1.30	-5.31
24-05-17	35.8	15.5	0.00	-2.21	24-05-17	34.9	18.3	0.04	-3.76	24-05-17	30.6	19.7	-0.72	-5.85
08-06-17	35.9	17.2	-0.16	-3.20	08-06-17	35.1	19.4	0.25	-2.99	08-06-17	26.2	20.1	-1.50	-6.44
22-06-17	35.8	19.1	-0.01	-2.61	22-06-17	35.4	20.6	0.20	-4.43	22-06-17	32.3	23.3	-0.26	-6.50
07-07-17	35.5	18.8	-0.01	-2.73	08-07-17	35.2	22.4	0.03	-4.43	08-07-17	28.3	21.7	-1.14	-6.84
21-07-17	36.1	19.8	-0.03	-3.00	21-07-17	35.3	21.2	0.19	-4.07	21-07-17	32.4	22.2	-0.34	-6.23
24-08-17	36.3	20.8	0.08	-3.82	24-08-17	35.5	21.5	0.26	-3.79	24-08-17	34.5	21.9	0.17	-3.99
18-09-17	34.9	18.8	-0.06	-4.17	18-09-17	32.6	19.1	-0.30	-5.29	18-09-17	24.7	17.7	-1.85	-7.75
21-10-17	35.5	18.4	0.06	-3.00	20-10-17	35.6	19.0	0.28	-2.68	20-10-17	32.9	18.8	-0.17	-5.06
03-11-17	36.2	16.5	0.08	-5.28	03-11-17	35.5	17.9	0.15	-4.13	03-11-17	33.4	17.3	-0.09	-5.21
18-11-17	36.1	15.4	0.08	-4.80	16-11-17	32.6	15.2	-0.44	-4.53	16-11-17	22.6	13.1	-2.12	-7.35
05-12-17	***14.8***	***13.3***	***-3.06***	***-10.81***	05-12-17	32.7	13.7	-0.33	-4.49	05-12-17	21.5	12.2	-2.31	-7.29
19-12-17	34.3	13.1	-0.20	-4.39	18-12-17	33.4	13.4	-0.23	-4.23	18-12-17	11.5	11.1	-4.16	-9.42
Mean	35.7	15.5	-0.03	-3.83	Mean	34.4	16.4	-0.04	-4.01	Mean	26.0	16.2	-1.57	-6.39
Minimum	34.3	11.7	-0.20	-5.59	Minimum	28.7	11.2	-1.24	-5.29	Minimum	1.7	10.0	-6.29	-11.66
Maximum	36.3	20.8	0.42	-2.21	Maximum	35.6	22.4	0.28	-2.68	Maximum	34.5	23.3	0.17	-3.99
Range	2.0	9.1	0.63	3.38	Range	6.9	11.2	1.52	2.62	Range	32.9	13.3	6.46	7.68

Table 2. Pearson correlation coefficients (r) among the physical and chemical water properties recorded at the three study localities.

	Berria Beach	Montehano	Carasa
Salinity-SST	0.28	0.46	0.59
p value	0.22	< 0.05	< 0.05
Salinity-$\delta^{18}O_w$	0.49	0.97	1.00
p value	< 0.05	< 0.05	< 0.05
Salinity-$\delta^{13}C_{DIC}$	0.18	0.66	0.93
p value	0.42	< 0.05	< 0.05
SST- $\delta^{18}O_w$	0.35	0.49	0.61
p value	0.11	< 0.05	< 0.05
SST-$\delta^{13}C_{DIC}$	0.45	0.13	0.38
p value	< 0.05	0.54	0.07
$\delta^{13}C_{DIC}$ - $\delta^{18}O_w$	0.23	0.63	0.92
p value	0.30	< 0.05	< 0.05

Table 3. Oxygen and carbon isotope values determined at the ventral margins of the shells collected throughout the year in Berria Beach and the corresponding reconstructed water temperatures (SST) using Eqs.1 and 2. SD = standard deviation among the ten specimens analysed from each collection event.

Collection date	$\delta^{18}O$ VPDB (‰)	SD	$\delta^{13}C$ VPDB (‰)	SD	Reconstructed SST (ºC)
14-12-16	1.20	0.16	-0.67	0.30	14.6
29-12-16	1.25	0.08	-0.95	0.47	14.4
12-01-17	1.43	0.10	-1.00	0.53	13.6
27-01-17	1.71	0.08	-1.16	0.82	12.4
10-02-17	1.61	0.25	-1.18	0.44	12.8
27-02-17	1.53	0.15	-1.03	0.53	13.2
10-03-17	1.25	0.11	-1.06	0.28	14.4
28-03-17	1.21	0.24	-1.38	0.37	14.5
25-04-17	1.34	0.20	-1.79	0.29	14.0
09-05-17	1.40	0.14	-1.43	0.29	13.7
24-05-17	1.22	0.11	-1.28	0.27	14.5
08-06-17	0.85	0.22	-0.87	0.38	16.1
22-06-17	0.66	0.17	-0.54	0.47	16.9
07-07-17	0.36	0.31	-0.45	0.45	18.2
21-07-17	0.19	0.14	-0.52	0.41	19.0
24-08-17	-0.12	0.07	-0.32	0.34	20.4
18-09-17	-0.09	0.14	-0.65	0.68	20.2
20-10-17	0.26	0.13	-0.75	0.56	18.7
03-11-17	0.30	0.11	-0.29	0.37	18.5
18-11-17	0.40	0.11	-0.30	0.30	18.0
19-12-17	0.88	0.30	-0.90	0.33	15.9
Mean	0.90		-0.88		15.9
Minimum	-0.12		-1.79		12.4
Maximum	1.71		-0.29		20.4
Range	1.83		1.50		8.0

Table 4. Summary of oxygen and carbon isotope values of the micromilled shells from Berria Beach (low and high intertidal zones), Montehano and Carasa. The $\delta^{18}O$ values from the Berria Beach specimens were used to reconstruct water temperatures (SST).

	Berria Beach (Low)			**Berria Beach (High)**			**Montehano**		**Carasa**	
	$\delta^{18}O_s$ VPDB (‰)	$\delta^{13}C_s$ VPDB (‰)	SST (℃)	$\delta^{18}O_s$ VPDB (‰)	$\delta^{13}C_s$ VPDB (‰)	SST (℃)	$\delta^{18}O_s$ VPDB (‰)	$\delta^{13}C_s$ VPDB (‰)	$\delta^{18}O_s$ VPDB (‰)	$\delta^{13}C_s$ VPDB (‰)
Mean	0.63	-0.38	17.0	0.77	-0.50	16.5	0.56	-1.02	-1.20	-3.62
Minimum	-0.65	-1.24	11.5	-0.70	-1.70	12.6	-1.31	-2.54	-1.98	-5.36
Maximum	1.93	1.09	22.8	1.67	0.06	23.1	1.87	-0.26	0.02	-2.15
Range	2.58	2.33	11.3	2.37	1.76	10.5	3.19	2.28	2.01	3.21

Table 5. Relationships between $\delta^{13}C_s$ and $\delta^{18}O_s$ values of *M. galloprovincialis* collected at the three study sites.

	r (Pearson)	Correlation slope	N
Berria Beach margins	-0.78	-1.10	21
Berria Beach (sequential)	-0.27	-0.38	162
Montehano	0.13	0.18	86
Carasa	0.56	0.41	91